Arch. Metall. Mater. **63** (2018), 4, 1769-1783

DOI: 10.24425/amm.2018.125104

Z. YAN-LING*, G. MING*#, L. FENG-SHAN*, Y. KAN*

ENRICHMENT, SEPARATION, AND RECOVERY OF PHOSPHORUS FROM DEPHOSPHORIZATION SLAG

A better understanding of phosphorus distribution in slag is necessary to develop an effective way to treat dephosphorization slag formed during steelmaking. Here, previous studies on the enrichment, separation, and recovery of phosphorus from dephosphorization slag are reviewed, along with their influencing factors. The results suggest that a proper heat treatment can promote the selective enrichment and growth of P-rich phases. Further, adding P_2O_5 and Fe_tO facilitates phosphorus enrichment. Also, $Ca_3(PO_4)_2$ is precipitated from slag containing 18 wt% P_2O_5. MnO and MgO in the slag barely affect the phosphorus recovery. In contrast, the addition of Al_2O_3 and TiO_2 significantly affects phosphorus enrichment and magnetic separation. A phosphorus recovery rate of more than 70% is achieved with the addition of 10 wt% Al_2O_3 or 10 wt% TiO_2. New phases ($Na_2Ca_4(PO_4)_2SiO_4$, Na_3PO_4, and $Ca_5(PO_4)_3F$) tend to be formed on the addition of Na_2O and CaF_2, which promote phosphorus enrichment. However, the addition of Na_2O and CaF_2 results in the incomplete separation of phosphorus and iron, as CaF_2 and Na_2O improve slag metallization and the magnetism of iron-rich phases.

Keywords: phosphorus enrichment, selective enrichment and growth, P-rich phase, magnetic separation

1. Introduction

Dephosphorization is a critical step in steelmaking. Dephosphorization slag based on CaO-Fe_tO-SiO_2 has high basicity (R) and Fe_tO content. However, the recycle/reuse of this slag is greatly limited by the circulation and enrichment of phosphorus, generating possible contamination in the liquid steel. Therefore, a better understanding of the phosphorus distribution and separating P are very important to promote the reutilization and treatment of dephosphorization slag formed during steelmaking.

Previous studies have proposed many methods of dephosphorization, such as gasification, addition of reductants [1], and floating separation [2]. Additionally, phosphorous is reduced and dissolved in liquid iron to decrease its content in slag [3]. However, few studies have focused on the effective recovery of phosphorus. Furthermore, the phosphorus content in slag is low (4-7%) and dispersed, making it difficult to recover phosphorus for other applications, such as the production of phosphate fertilizers [4]. Therefore, it is necessary to promote the enrichment, growth, and effective recovery of phosphorus from dephosphorization slag. Sui [5-6] has proposed the selective enrichment and separation of phosphorus based on the extraction of valuable components. According to this mechanism, by selectively gathering the dispersed components in the target phase, the efficiency of separating valuable components increases. Similarly, phosphorus is selectively gathered in the P-rich phase. This process improves the enrichment rate and separation efficiency of phosphorus. Most recent studies [7-12] have focused on the effect of slag basicity, slag composition (MgO, MnO, P_2O_5, Fe_tO), and additives (Na_2O, CaF_2, Al_2O_3, TiO_2) on the selective enrichment, growth, and separation of phosphorus along with the mechanism of phosphorus enrichment [18-21]. However, most of the above studies have focused on laboratory investigations. Therefore, research on the resource utilization of P in industrial production is scarce.

To effectively recycle Fe and P of dephosphorization slag, the effects of slag basicity, slag composition, and additives on the enrichment, separation, and recovery of phosphorus are reviewed. Besides, the challenges and factors associated with "phosphorus enrichment and growth – separation – recycling" have been considered.

2. Properties of dephosphorization slag

2.1. Phase structure of dephosphorization slag

CaO-Fe_tO-SiO_2 slag consists of a P-rich phase, matrix phase, and RO phase [18,19]. As shown in Fig. 1, the P-rich phase in the slag is mainly in the form of a $n Ca_2SiO_4 \cdot Ca_3(PO_4)_2$ solid solution (nC_2S-C_3P) and the P_2O_5 content in this solid solution is more than 20% [20,21]. The white RO phase is mainly composed of iron oxides or Fe-Mn oxides. Extra phosphorous is present in the matrix phase.

* UNIVERSITY OF SCIENCE AND TECHNOLOGY BEIJING, STATE KEY LABORATORY OF ADVANCED METALLURGY BEIJING 100083, CHINA

Corresponding author: gaoming0309@163.com

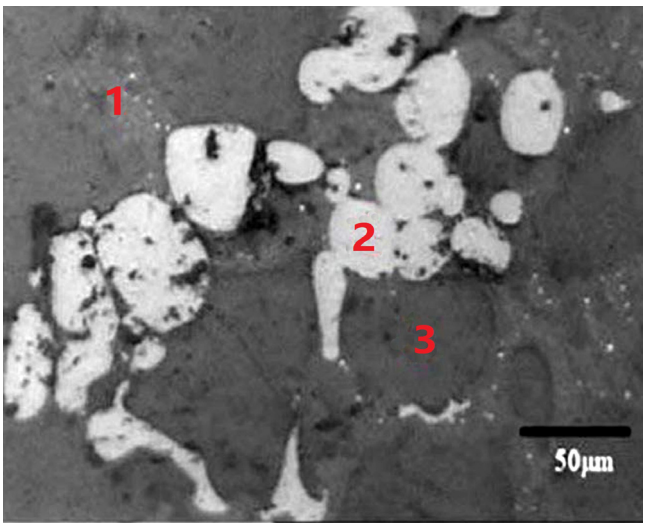

Fig. 1. Main phases in slag (1: matrix phase, 2: RO phase, 3: P-rich phase) [19]

2.2. Factors influencing phase structure

2.2.1. Slag Basicity

Slag basicity mainly affects the formation of xCaO·SiO$_2$ phase. Then the following phenomenon will happen. Firstly, the C_3S phase is formed in high-basicity slag [8]. Meanwhile, the C_3S reacts with P_2O_5 and CaO in slag to form nC$_3$S-C$_3$P. With decreasing slag basicity, the C_3S content decreases and the C_2S phase is formed. Similarly, solid C_2S particles dissolve in the slag, and the nC$_2$S-C$_3$P phase is generated. Subsequently, the C_2S phase disappears in low-basicity slag, and a new CS phase is generated, which leads to a decrease in the nC$_2$S-C$_3$P content. The P_2O_5 content in the phases gradually increases in the order of nC$_3$S-C$_3$P < nC$_2$S-C$_3$P < C$_3$P [8,36].

Lin [8] has analyzed the influence of SiO_2 modification on phosphorus enrichment in P-bearing steelmaking slag (P_2O_5 = 10 wt%). According to Fig. 2a, C_3S appears at R = 4 and disappears when R = 1-3. Then, C_2S and nC$_2$S-C$_3$P are formed at 1623 K (R = 2.5) as shown in Fig. 2b-d. Finally, CS is formed when R < 1.5. Son [36] has also reported that nC$_2$S-C$_3$P is generated in CaO-Fe$_t$O-SiO$_2$-5 wt% P_2O_5 slag (Fe$_t$O = 15-20 wt %) at R = 1 and R = 1.5. Therefore, the optimal basicity for generating nC$_2$S-C$_3$P is 1.5-2.5. Under favorable dynamics conditions, more P_2O_5 accumulates near C_2S particles at higher temperatures [31]. Therefore, the phosphorus content in the P-rich phase at 1400°C is higher than that at 1350°C [15].

2.2.2 Slag Composition

Previous studies have reported that MnO and MgO mainly enter into the RO phase to form $MgFe_2O_4$ and $MnFe_2O_4$, and different P_2O_5 and Fe$_t$O contents affect the form of the C$_x$S phase [9-11,36].

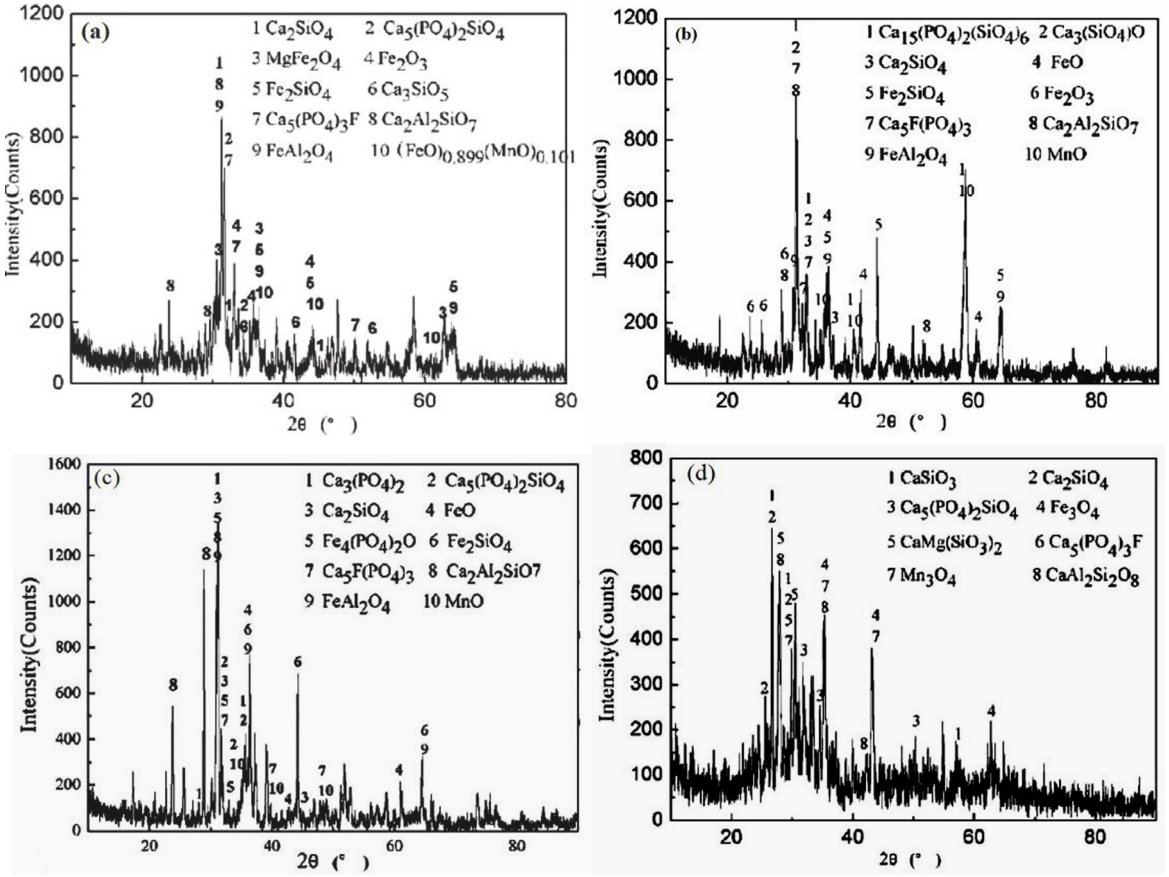

Fig. 2. X-ray diffraction patterns (a: R = 4, b: R = 3, c: R = 2, d: R = 1) [8]

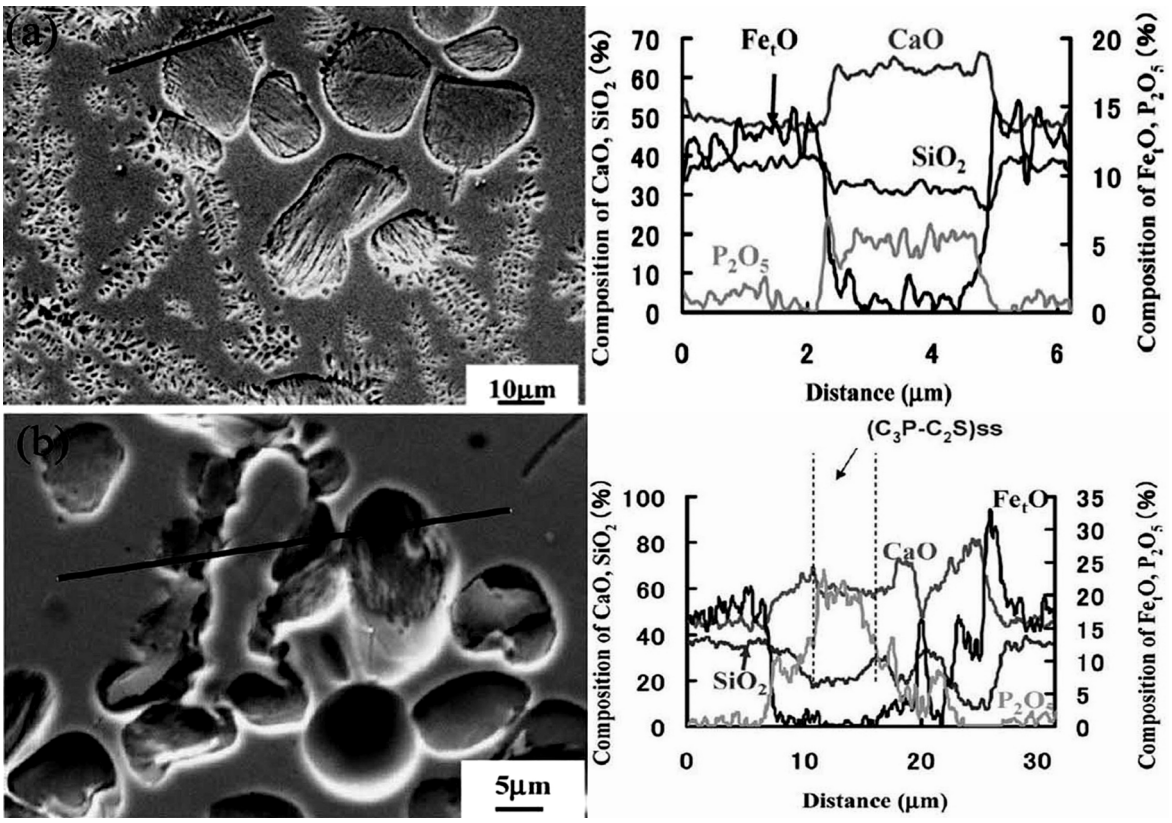

Fig. 3. Results of SEM and line scanning (a: 10 wt% Fe_tO, b: 15 wt% Fe_tO) [36]

Son [36] has reported the effect of elemental compositions on CaO-Fe_tO-SiO_2-5 wt% P_2O_5 slag (CaO/SiO_2 = 1.5). Fig. 3a shows that CS and C_2S are generated at Fe_tO = 10 wt%. However, according to Fig. 3b, C_3P and nC_2S-C_3P are formed when the Fe_tO content is high (Fe_tO = 15-20 wt%).

Compared with Fe_tO, the initial P_2O_5 content in the slag changes the form of the P-rich phase [7,9-11]. Li [7] has examined the behavior of phosphorus enrichment in CaO-FeO-Fe_2O_3-SiO_2-P_2O_5 slag and has found that the initial P_2O_5 content promotes the generation of nC_2S-C_3P. Meanwhile, C_3P is formed when more than 18 wt% P_2O_5 is added [9-11]. The results in Fig. 4 show that $CaO_{15}(P_2O_5)_2(SiO_2)_6$ is generated with the addition of less than 18 wt% P_2O_5, and C_3P is formed when the P_2O_5 content is up to 18 wt%. C_3P has lower Gibbs free energy than C_2S; therefore, it is more stable in the temperature range 400-1800°C. Further, compared to SiO_2, P_2O_5 can more easily combine with CaO. Hence, CaO preferentially combines with P_2O_5 and C_3P is formed [9].

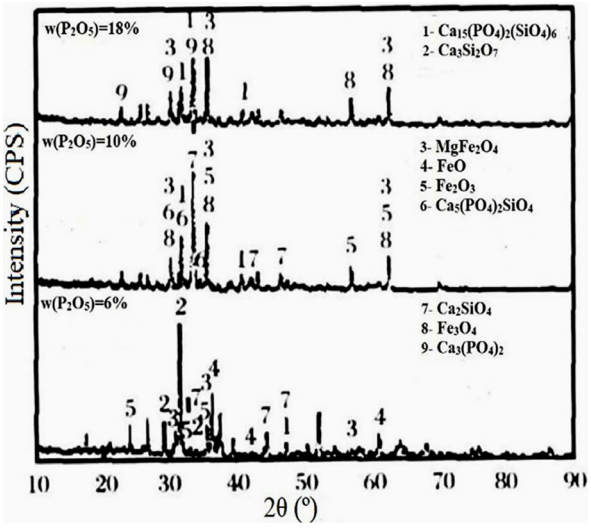

Fig. 4. Effect of P_2O_5 content on precipitated phase [9]

In summary, MgO and MnO have little effect on the P-rich phase. Appropriate P_2O_5 and Fe_tO contents promote the precipitation of the P-rich phase. nC_2S-C_3P and C_3P are formed with the addition of more than 15 wt% Fe_tO and 18 wt% P_2O_5, respectively.

2.2.3. Addition of CaF_2 and Na_2O

Many studies have shown that adding CaF_2 and Na_2O changes the primary phase and phosphorus form, respectively [40,41]. Fig. 5 shows that $6C_2S$-C_3P and C_2S-C_3P are generated in fluorine-free modified slag. A new phase, $Ca_5(PO_4)_3F$, is generated on the addition of 6 wt% CaF_2. Therefore, the nC_2S-C_3P and $Ca_5(PO_4)_3F$ phases are mainly considered to be P-rich phases [40]. Fig. 6 shows that Na_2O-free modified slag consists of $6C_2S$-C_3P, C_2S-C_3P, C_2S, and RO phases. However, $Na_2Ca_4(PO_4)_2SiO_4$ is formed in Na_2O-bearing slag. Meanwhile, Na_3PO_4 is generated in slag containing 6 wt% Na_2O [41].

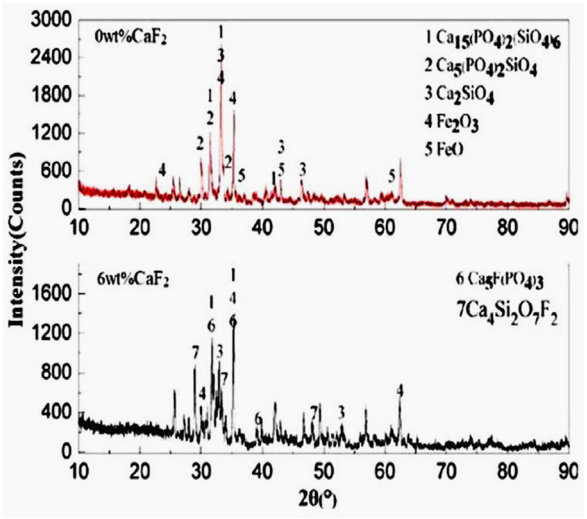

Fig. 5. CaF_2-modified slag [40]

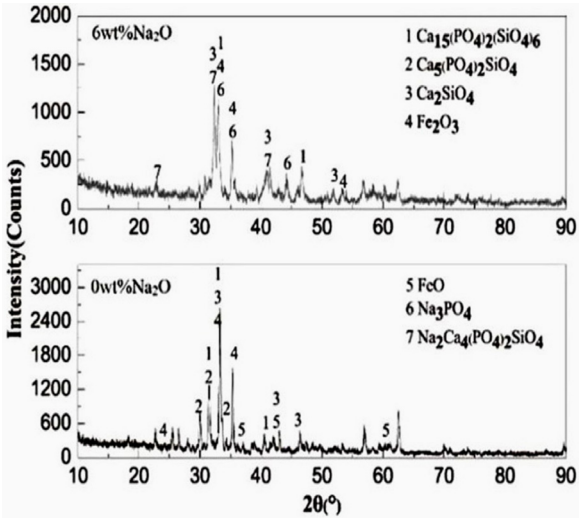

Fig. 6. Na_2O-modified slag [41]

2.2.4. Addition of Al_2O_3 and TiO_2

Most studies have revealed that Al_2O_3 and TiO_2 modification are beneficial to increase the phosphorus content in the P-rich phase [42-45]. Jiang [43] has examined the effect of Al_2O_3 on the phosphorus form existing in CaO-SiO_2-10 wt% FeO-6 wt% MgO-4 wt% MnO-10 wt% P_2O_5-Al_2O_3 slag. According to Fig. 7b, $Ca_2Al_2SiO_7$ is generated in Al_2O_3-bearing slag, along with the matrix, RO, and P-rich phases. Further, C_3P is formed on adding 11 wt% Al_2O_3.

Lin [45] has reported the effect of TiO_2 modification on phosphorus enrichment in industrial slag by adding 10 wt%

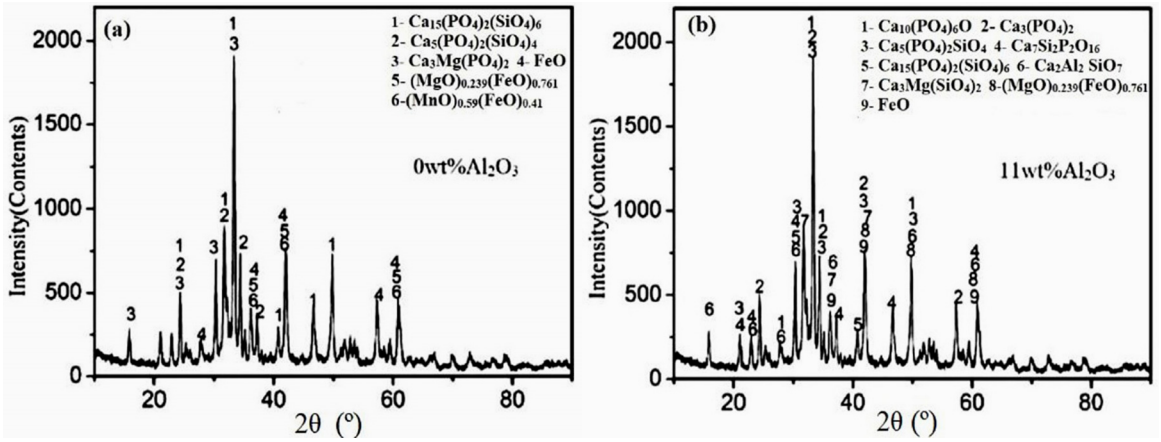

Fig. 7. X-ray diffraction patterns of Al_2O_3-modified slag [43]

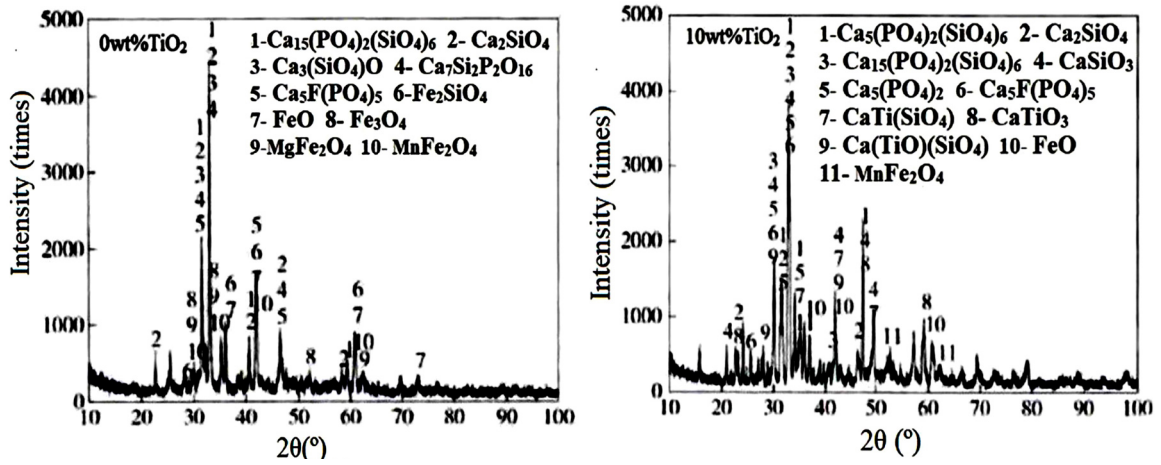

Fig. 8. X-ray diffraction patterns of TiO_2-modified slag [45]

P_2O_5. As shown in Fig. 8a, TiO_2-free modified slag consists of the matrix, RO, and $CaO_{15}(P_2O_5)_2(SiO_2)_6$ phases. However, new phases ($CaTiO_3$, $CaSiTiO_4$) are generated after adding 10 wt% TiO_2 (Fig. 8b). $[TiO_6]$, an important part of $MgFe_2O_4$-Mg_2TiO_4 and $CaTiO_3$, is formed after adding TiO_2. Furthermore, $[TiO_4]$ and $[SiO_4]$ can be copolymerized to form $CaSiTiO_4$, and C_2S in nC_2S-C_3P is robbed $CaSiTiO_4$ to generate yC_2S-C_3P ($y < n$) [4]. Therefore, new phases are generated on adding Al_2O_3 and TiO_2.

2.2.5. Temperature and cooling conditions

Su [33] has reported the distribution of phase structure in CaO-SiO_2-Fe_tO-P_2O_5 slag under 1350°C and 1400°C. After holding 600s, the slag consists of C_2S-C_3P phase and matrix phase. However, Fig. 9 shows that C_2S-C_3P phase is blocked under 1350°C. Therefore, the lower temperature promotes the enrichment of P_2O_5.

In addition, the cooling conditions have effect on phase structure. Li [18] has reported the P-rich phase in steel slag under water quench process and hot splash process. The P-rich phase under water quench process is nC_2S-C_3P, while it is C_3P under hot splash process.Wu [23] has reported the distribution in SiO_2 modified slag. The results show that P is gathered to C_2S phase when the cooling rates are $1°C \cdot min^{-1}$ and $3°C \cdot mmin^{-1}$. The C_2S phase are spherical and arborization. However, the C_2S phase is arborization and punctate when the cooling rate is $5°C \cdot min^{-1}$.

3. Phosphorus enrichment in dephosphorization slag

3.1 Mechanism of phosphorus enrichment

The mechanism of phosphorus enrichment can be concluded from the following process. First, solid C_2S particles dissolve in the slag. Then nC_2S-C_3P is generated in the multi-phase area where solid and liquid phases coexist. Finally, the solid-solution layer is extended and completely changes into the nC_2S-C_3P layer with the shrinking of the solid C_2S particles [21-27].

According to the slag ionic structure theory [22], slag consists of oxides, compounds, and charged protons (ions). As the SiO_2 content in basic dephosphorization slag is higher than the P_2O_5 and Al_2O_3 contents, C_2S and C_3S based on SiO_4^{4-} are generated during solidification, and SiO_4^{4-} is more easily replaced by P_2O_5 and Al_2O_3. Then, phosphorus is precipitated as PO_4^{3-} and coexists with SiO_4^{4-}. Therefore, it is difficult to generate C_3P in dephosphorization slag. The formation reaction of nC_2S-C_3P can be expressed as Eq. (1).

$$2nCaO + nSiO_2 + Ca_3(PO_4)_2 = nCa_2SiO_4 \cdot Ca_3(PO_4)_2 \quad (1)$$

It is well known that C_3S and C_2S react with C_3P to form a solid solution. Hence, the phosphorus in the slag is distributed in multiple phases [23]. Stable C_3S changes to spherical C_2S at 1300°C. Therefore, the P-rich phase mainly occurs in the $nC_2S \cdot C_3P$ phase as C_3S cannot react with C_3P at any ratio.

Most researchers have reported the behavior of mass transfer between single C_2S particles and slag [24-27]. C_2S particles are regarded as a multi-layered filter paper. Here the phosphorus in the slag is filtered and the phosphorus content gradually decreases in the direction of the C_2S particles. Therefore, nC_2S-C_3P is generated until the C_2S particles disappear. Fig. 10 shows the reaction between C_2S particles and CaO-SiO_2-Fe_tO-P_2O_5 slag at 1500°C for 300 s. It reveals that a solid-solution layer is formed between the slag and the C_2S particles after 1 s (Fig. 10a), and after 60 s (Fig. 10b-c), the number of C_2S particles decrease with increasing area of this solid-solution layer [27]. Ono [24] has reported that ferrous and iron oxides increase the activity coefficient of C_3P in CaO-SiO_2-FeO/Fe_2O_3 slag. Most of the P_2O_5 in the slag reacts with C_2S particles to generate a solid solution. Moreover, the products float to the top of the slag. Ito [25] has measured the distribution ratio between CaO-SiO_2-FeO/Fe_2O_3 slag and C_2S particles. The results reveal that 80% P_2O_5 is transferred from the slag to the surface of the C_2S particles to form nC_2S-C_3P. Wang [26] has analyzed the enrichment be-

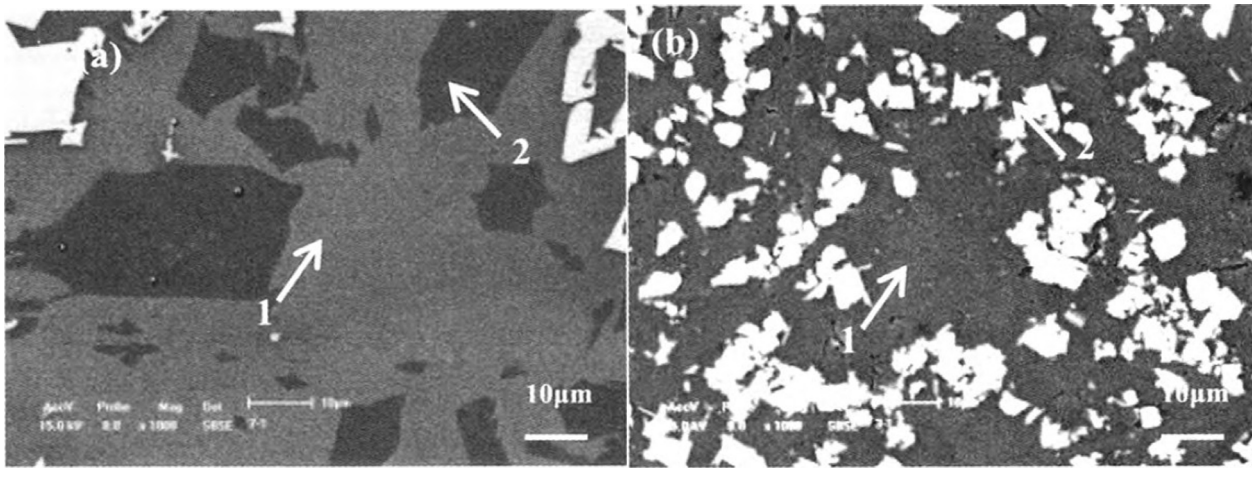

Fig. 9. The phase structure at different temperatures:(a)1350°C and (b) 1400°C (1: matrix phase, 2: P-rich phase) [33]

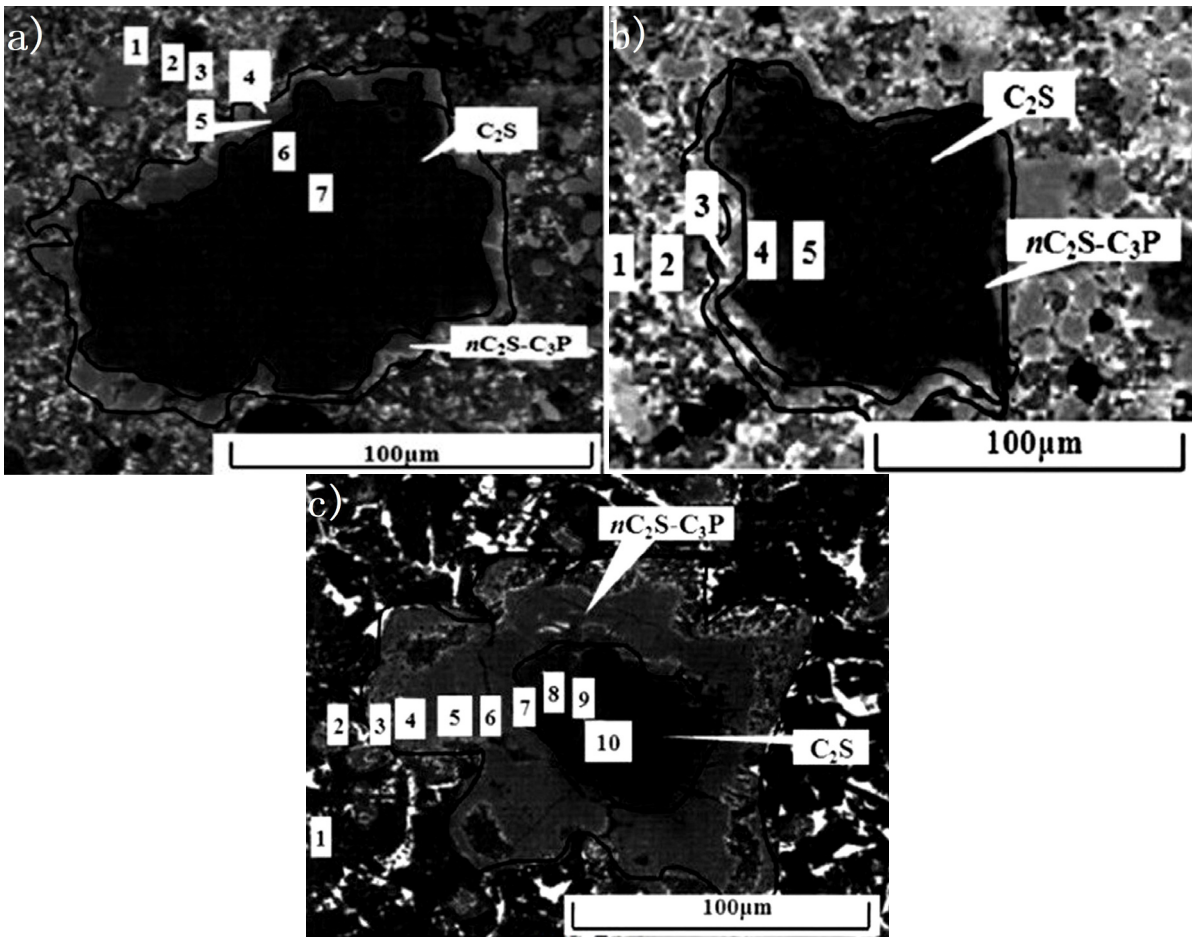

Fig. 10. SEM results at different times: (a)1s, (b)60s, and (c)300s [27]

havior of CaO-SiO_2-Fe_tO-P_2O_5 slag at 1400°C and has found that C_2S particles provide space for phosphorus enrichment. Therefore, phosphorus diffuses from the slag to the surface of the C_2S particles.

Furthermore, a macro-process for phosphorus enrichment has been proposed . Yang et. all [28-30] have reported the reaction between C_2S particles and CaO-SiO_2-FeO_x-P_2O_5 slag at 1400°C for 60 s. The mechanism is illustrated in Fig. 11.

1) C_2S particles dissolve into the slag and the slag penetrates into the solid sample (Fig. 11a).
2) The edge of the solid C_2S particles changes into a multi-phase area where solid and liquid phases coexist (Fig. 11b).
3) In this multi-phase area, CaO and P_2O_5 react with the C_2S particles to form $n$$C_2S$-$C_3P$ (Fig. 11c).
4) The multi-phase area shifts toward the side of the C_2S particles to form a new P-rich phase (Fig. 11d).
5) The previously formed P-rich phase is either retained (Fig. 11e1), partly dissolved (Fig. 11e2), or fully dissolved into the slag (Fig. 11e3). The P-rich phase region is gradually extended.

Suito [31] has examined the behavior of phosphorus diffusion from CaO-Fe_tO-P_2O_5(-SiO_2) slag to CaO particles at 1400°C. The results show that $n$$C_2S$-$C_3P$ is generated at the surface of CaO particles within 30 s. After 5 min, CaO-Fe_tO is produced between the $n$$C_2S$-$C_3P$ and CaO particles. Inoue [32] has reported the phosphorus distribution between CaO-Fe_tO-P_2O_5 slag and C_2S particles. The results show that all the phosphorus in C_2S particles (20-50 μm) is converted into nC_2S-C_3P in less than 5 s. Only the rim part of the particles (5 μm) and the small particles (3-8 μm) change to $n$$C_2S$-$C_3P$ within 5 s when the particles are clustered. However, this phenomenon is not observed in CaO-SiO_2-Fe_tO-P_2O_5 slag.

Consequently, the formation of the P-rich phase can be described by the following process. The phosphorus in the slag transfers to the C_2S particles at high temperatures and reacts with C_2S to generate $n$$C_2S$-$C_3P$, and the previously formed P-rich phase is replaced by new products.

3.2. Factors influencing selective enrichment

3.2.1. Concept of Selective Enrichment

Temperature and the size of the C_2S particles affect phosphorus enrichment [26,33]. Because a higher temperature improves the kinetics of slag formation, the phosphorus content in the P-rich phase at 1400°C is higher than that at 1350°C [26,33]. The size of the P-rich phase increases with increasing enrichment time [33], and C_2S particles, of size less than 50 μm, are completely converted to form a P-rich phase [26].

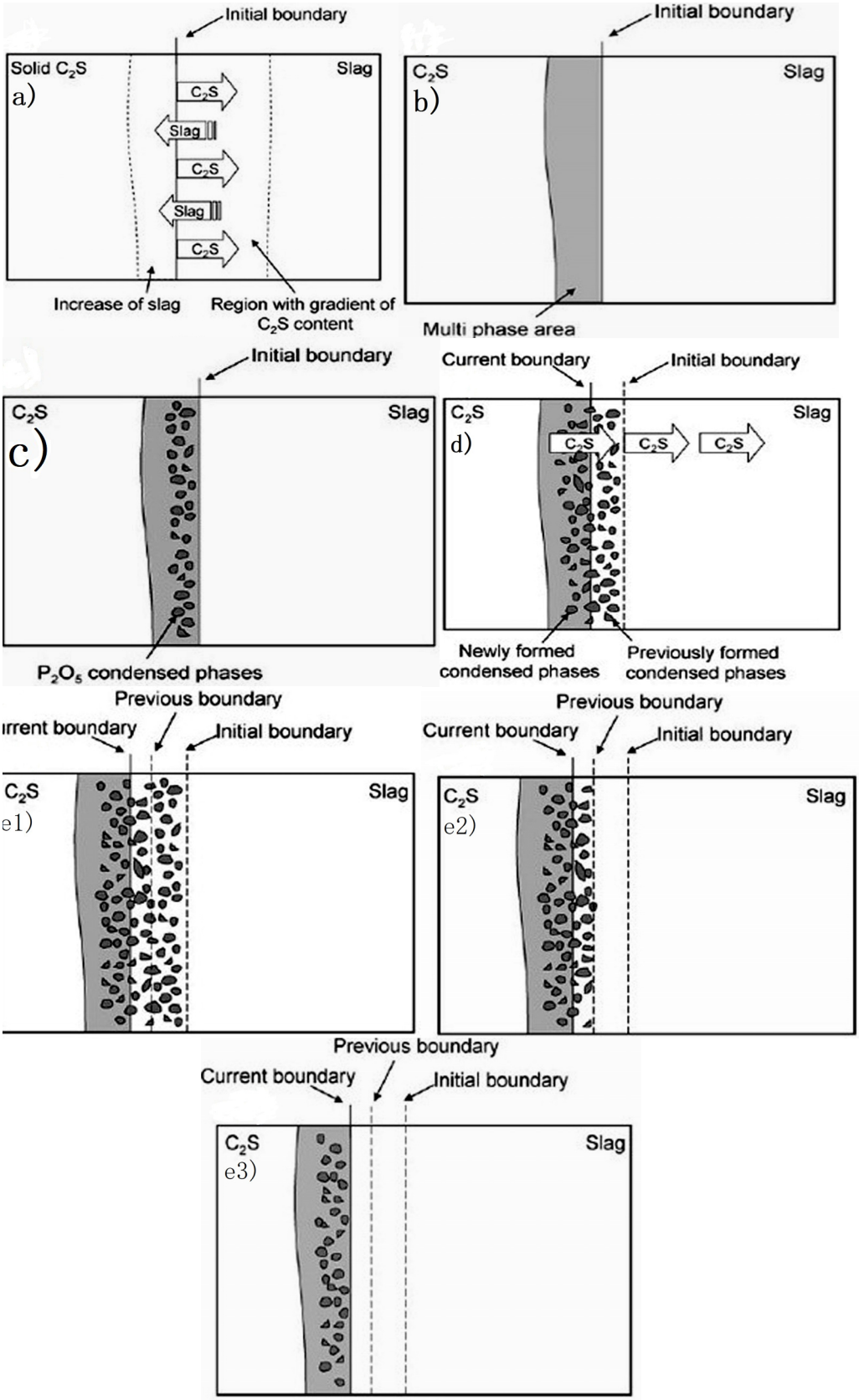

Fig. 11. Formation mechanism of $n$$C_2S$-$C_3P$ [28]

However, the phosphorus content in the P-rich phase is low and dispersed. Therefore, the selective enrichment of P is important to increase the enrichment, separation, and recovery of the P-rich phase [34,35]. In 1978, Jha [34] proposed the concept of selective precipitation to obtain nickel sulfide and cobalt sulfide. In China, Sui [35] has proposed the technology of selective enrichment and separation. “Selective enrichment” means that suitable thermodynamics and kinetics are achieved by changing

the slag compositions and additives. Then, valuable components interspersed in each phase are selectively transferred. Eventually, the valuable components accumulate in the target phase due to chemical gradient. The slag basicity and composition, the initial content of P_2O_5, and the value of (%FeO)/(%CaO) have effect on the selective enrichment.

3.2.2. Slag Basicity and Composition

Using a suitable slag basicity is a good method to promote selective enrichment. Zhou [11] has examined the behavior of distribution of phosphorus between the P-rich phase and the matrix phase. The results show that phosphate capacities increase with decreasing slag basicity. According to Fig. 12, the P_2O_5 content in the P-rich phase decreases with increasing slag basicity. Lin [8] has reported the influence of SiO_2 modification on the phosphorus enrichment in P-bearing steelmaking slag. The results show that the P_2O_5 contents in the P-rich phase were 19-25 wt%, 31-32 wt%, 32-33 wt%, and 34-37 wt% for R values decreasing from 4 to 1, respectively. Son [36] has analyzed CaO-20 wt% Fe_tO-SiO_2-5 wt% P_2O_5 slag and has found that the P_2O_5 content was 37.3 wt% and 22.7 wt% at R = 2.0 and R = 2.5, respectively. Thus, a higher slag basicity is harmful to phosphorus enrichment.

Many studies have reported the effect of slag compositions (MgO, MnO, P_2O_5, Fe_tO) on the selective enrichment of the P-rich phase. The addition of P_2O_5 increases the phosphorus content in the P-rich phase, whereas MgO and MnO have little effect [9-11,15,36-39].

Fe_tO is an inevitable component in slag and reduces polymerization and viscosity. Additionally, it contributes to mass transfer and phosphorus enrichment in dephosphorization slag [4]. Son [36] has analyzed the effect of Fe_tO on CaO-Fe_tO-SiO_2-5 wt% P_2O_5 slag. As shown in Fig. 13, the P_2O_5 content in the P-rich phase is 17.6 wt% and 22.7 wt% with the addition of 10 wt% Fe_tO and 20 wt% Fe_tO, respectively. Moreover, the common effect of Fe_tO and CaO on slag is unclear [7,37,38]. Li [7] has analyzed the effect of Fe_tO/CaO content on CaO-FeO-Fe_2O_3-SiO_2-P_2O_5 slag and found that $n$$C_2S$-$C_3P$ decreases with increasing Fe_tO/CaO content.

Zhou [9] has reported the effect of initial P_2O_5 content on phosphorus enrichment in CaO-Fe_tO-SiO_2-P_2O_5 slag. According to Figure 12, when the P_2O_5 content is increased from 6 wt% to 8 wt%, the phosphorus content in the P-rich phase increases from 20.33 wt% to 33.99 wt% and reaches a maximum value (34.91 wt%) when 18 wt% P_2O_5 is added. This suggests that phosphorus content in the P-rich phase increases with increasing initial P_2O_5 content.

$MgFe_2O_4$ and $MnFe_2O_4$ generated by MgO, MnO, and Fe_2O_3 enter into the RO phase, as shown in Eq. (2) [11,15,39]. Lin [15] has analyzed the effect of MgO and MnO on phosphorus enrichment in CaO-SiO_2-30wt%Fe_2O_3-MgO-MnO-10wt%P_2O_5 slag. According to Figure 12, when the MgO content increases from 5 wt% to 10 wt%, the P_2O_5 content in the P-rich phase changes from 20.76 wt% to 19.66 wt%. Similarly, when the MnO content increases from 5 wt% to 10 wt%, the P_2O_5 changes from 22.62 wt% to 19.66 wt%. Thus, P_2O_5 content in the P-rich phase does not change significantly.

$$MgO + Fe_2O_3 = MgFe_2O_4$$
$$MnO + Fe_2O_3 = MnFe_2O_4 \quad (2)$$

In summary, MgO and MnO have little effect on the selective enrichment of the P-rich phase. In contrast, the P_2O_5 content in the P-rich phase reaches 20 wt% and 35 wt% on the addition of 15 wt% Fe_tO and 18 wt% P_2O_5, respectively.

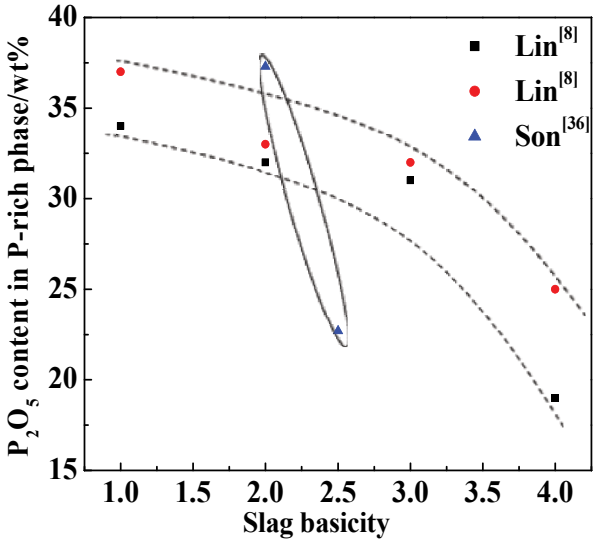

Fig. 12. Effect of slag basicity on P_2O_5 content

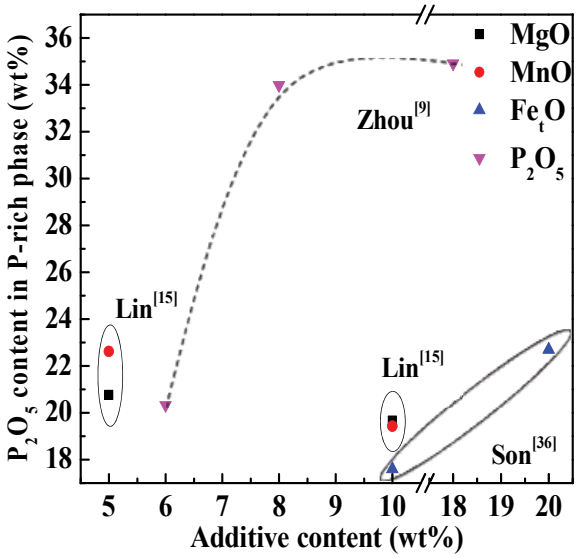

Fig. 13. Effect of slag composition on P_2O_5 content

3.2.3. Addition of CaF_2 and Na_2O

CaF_2 and Na_2O can significantly reduce the melting point of slag and promote phosphorus enrichment [4,11,40,41]. Wang [4] has analyzed the effect of CaF_2 on crystallization in CaO-

SiO_2-Fe_tO-MgO-P_2O_5-CaF_2 slag. The results show that the P_2O_5 content in $Ca_5(PO_4)_3F$ reduces to 28.35 wt% with the addition of 3 wt% CaF_2. According to Fig. 14, on adding 3 wt% CaF_2 into the slag, the P_2O_5 content in the P-rich phase is 32.5 wt%, and on adding 6 wt% CaF_2 into the slag, the P_2O_5 content in the P-rich phase increases to 35.65 wt% [11]. Meanwhile, Lin [40] has reported the phosphorus enrichment behavior in CaO-SiO_2-Fe_tO-MgO-P_2O_5-CaF_2 slag. The results reveal that the P_2O_5 content in the P-rich phase is 20.75 wt% in fluorine-free modified slag. On increasing the CaF_2 content from 3 wt% to 6 wt%, the P_2O_5 content in the P-rich phase increases from 34.0 wt% to 37.75 wt%. Furthermore, it is necessary to control the CaF_2 content to avoid lining erosion and environmental pollution.

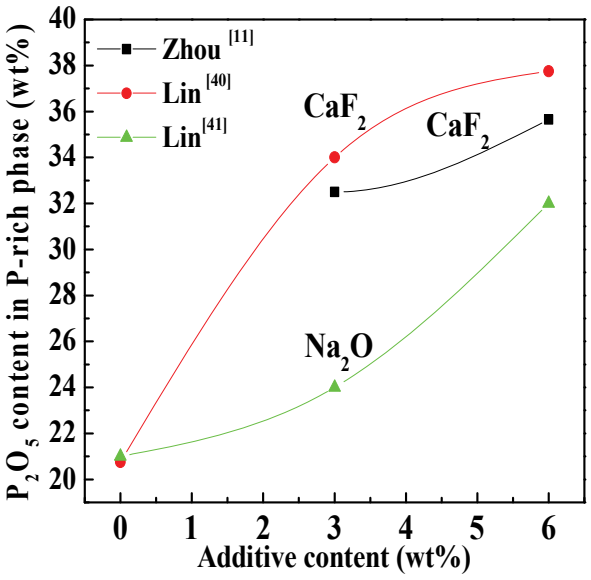

Fig. 14. Effect of addition of CaF_2 and Na_2O on selective enrichment of phosphorus

The form of phosphorus in the P-rich phase changes on the addition of Na_2O according to Eqs. (3-5) [41].

$$12CaO + 6SiO_2 + Ca_3(PO_4)_2 = 6Ca_2SiO_4 \cdot Ca_3(PO_4)_2 \quad (3)$$

$$Na_2O + 6Ca_2SiO_4 \cdot Ca_3(PO_4)_2 = Na_2Ca_4(PO_4)_2SiO_4 + 5Ca_2SiO_4 + CaO \quad (4)$$

$$3Na_2O + Na_2Ca_4(PO_4)_2SiO_4 = 2Na_3PO_4 + Ca_2SiO_4 + 2CaO \quad (5)$$

As shown in Eq. (3), $6C_2S$-C_3P is precipitated in the previous stage of cooling. Then $Na_2Ca_4(PO_4)_2SiO_4$ is generated by the reaction of $6C_2S$-C_3P and Na_2O at 1623 K (Eq. (4)). Moreover, Na_3PO_4 is formed in the presence of excess Na_2O content (Eq. (5)). Lin [41] has reported the influence of Na_2O on phosphorus enrichment in CaO-SiO_2-Fe_tO-MgO-P_2O_5 slag. As shown in Fig. 14, the P_2O_5 content in the P-rich phase is 21 wt% in Na_2O-free modified slag. When the Na_2O content is increased from 3 wt% to 6 wt%, the P_2O_5 content in the P-rich phase increases from 24 wt% to 32 wt%. According to the slag ionic structure theory, the combination of Na^+ and phosphorus ions is stronger than that of Ca^{2+} and phosphorus ions. Moreover, Ca^{2+} in $6C_2S$-C_3P or $Na_2Ca_4(PO_4)_2SiO_4$ is replaced by Na^+. Further, Na_3PO_4 is generated when sufficient Na_2O is added.

Thus, the P_2O_5 content in the P-rich phase increases to 30 wt% on adding 3 wt% CaF_2 or 6 wt% Na_2O. Furthermore, considering the limitations of CaF_2, it can be replaced by Na_2O to promote the selective enrichment of phosphorus.

3.2.4. Addition of Al_2O_3 and TiO_2

Previous studies have shown that Al_2O_3 and TiO_2 modification are beneficial to phosphorus enrichment [42-45]. The mechanism of Al_2O_3 modification can be illustrated as shown in Eqs. (6-7) [42-44].

$$m Ca_2SiO_4 \cdot Ca_3(PO_4)_2 + n Al_2O_3 = n Ca_2Al_2SiO_7 + y Ca_2SiO_4 \cdot Ca_3(PO_4)_2 \quad (6)$$

$$y Ca_2SiO_4 \cdot Ca_3(PO_4)_2 + x Al_2O_3 = x Ca_2Al_2SiO_7 + (y - x) Ca_2SiO_4 \cdot Ca_3(PO_4)_2 \quad (7)$$

First, mC_2S-C_3P is precipitated at 1623 K and gradually decreases with the generation of yC_2S-C_3P ($y < n$) (Eq. (6)). Then $(y - x)C_2S$-C_3P is produced on adding Al_2O_3 (Eq. (7)). Finally, C_2S in yC_2S-C_3P disappears when the Al_2O_3 content is sufficient to make $y = x$, and C_3P is precipitated from the slag.

As shown in Fig. 15, Diao [44] has revealed that the P_2O_5 content in the P-rich phase reached 5.1 wt% on adding 8 wt% Al_2O_3 into CaO-SiO_2-10wt%FeO-MgO-MnO-P_2O_5 slag ($R = 2$), whereas the content increases to 9.15 wt% on adding 11 wt% Al_2O_3. Wang [4] has also reported that the P_2O_5 content in the P-rich phase reaches 28.71 wt% with the addition of 15.17 wt% Al_2O_3 in CaO-SiO_2-Fe_tO-MgO-P_2O_5 slag.

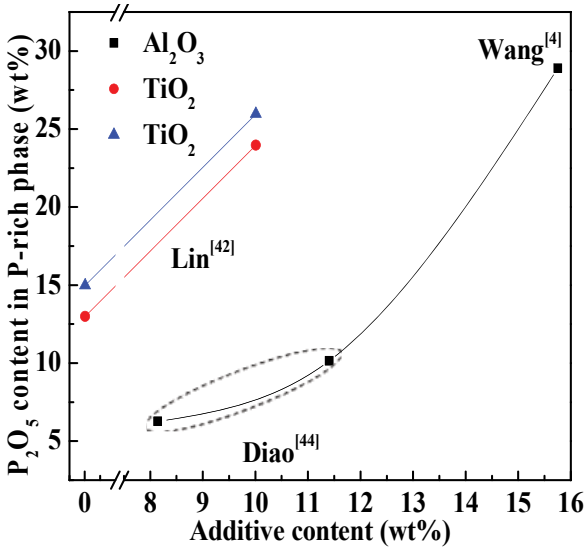

Fig. 15. Effect of addition of Al_2O_3 and TiO_2 on selective enrichment of phosphorus

Similarly, the mechanism of TiO_2 modification is shown in Eqs. (8-9) [45]. $CaSiTiO_5$ and $CaTiO_3$ are generated on adding TiO_2. Lin [45] has found that the P_2O_5 content in the P-rich phase is only 13-15 wt% and increases to 24-26 wt% on adding 10 wt% TiO_2.

$$\begin{aligned} m\mathrm{Ca_2SiO_4\cdot Ca_3(PO_4)_2} + 2n\mathrm{TiO_2} \\ = n\mathrm{Ca_2SiTiO_5} + n\mathrm{CaTiO_3} \\ + y\mathrm{Ca_2SiO_4\cdot Ca_3(PO_4)_2} \end{aligned} \quad (8)$$

$$\begin{aligned} y\mathrm{Ca_2SiO_4\cdot Ca_3(PO_4)_2} + 2x\mathrm{TiO_2} \\ = x\mathrm{Ca_2SiTiO_5} + x\mathrm{CaTiO_3} \\ + (y-x)\mathrm{Ca_2SiO_4\cdot Ca_3(PO_4)_2} \end{aligned} \quad (9)$$

The effect of Al_2O_3 and TiO_2 on the selective enrichment of the P-rich phase is significant. The P_2O_5 content in the P-rich phase reaches 20 wt% on adding 15 wt% Al_2O_3 or 10 wt% TiO_2 to the slag.

4. Selective growth and precipitation in dephosphorization slag

4.1. Effect of temperature on selective growth and precipitation

According to the mechanism of selective enrichment and separation by Sui, the enrichment phase will grow up by controlling temperature, slag basicity , slag composition, and additives. Finally, the efficiency of separating valuable components is improved. The process is called as selective growth.

Heat treatment is the main factor affecting selective growth and precipitation. Most reports agree that the P-rich phase is thicker at lower cooling rates [4,5,7,23,47].

Wang [4] has analyzed the crystallization of the P-rich phase in $CaO\text{-}SiO_2\text{-}Fe_tO\text{-}MgO\text{-}P_2O_5\text{-}Al_2O_3/TiO_2$ slag by differential scanning calorimetry. The results reveal that the crystallization temperature of the P-rich phase increases with decreasing cooling rate. The diffusion of the P-rich phase is hampered at higher sub-cooling degrees. Li [7] has reported the effect of temperature on selective growth in $CaO\text{-}FeO\text{-}Fe_2O_3\text{-}SiO_2\text{-}P_2O_5$ slag. The results reveal that the size of the P-rich phase and its crystal fraction are 40 μm and 24% at a cooling rate of 3°C/min, respectively, and the latter reaches its maximum value within 1 h. Wu [23] has examined the average size of P-rich phases in industrial SiO_2-modified slag. On decreasing the cooling rate from $5°C\cdot min^{-1}$ to $3°C\cdot min^{-1}$ and $1°C\cdot min^{-1}$, the average size increases from 8 μm to 56 μm and 87 μm and the P_2O_5 content in the P-rich phase increases from 3.65 wt% to 7.5 wt% and 7.74 wt%, respectively. Yang [47] has analyzed the growth of the P-rich phase in $CaO\text{-}SiO_2\text{-}Fe_2O_3\text{-}MgO\text{-}MnO\text{-}P_2O_5\text{-}Al_2O_3\text{-}TiO_2$ slag at 1520°C. The statistical results show that the relationship between holding time (t) and the size of the C_2S layer (D) can be described by $D = kt^m$. Where, k and m is constant. Thus, the size of the P-rich phase exceeds 40 μm when the cooling rate is less than $3°C\cdot min^{-1}$.

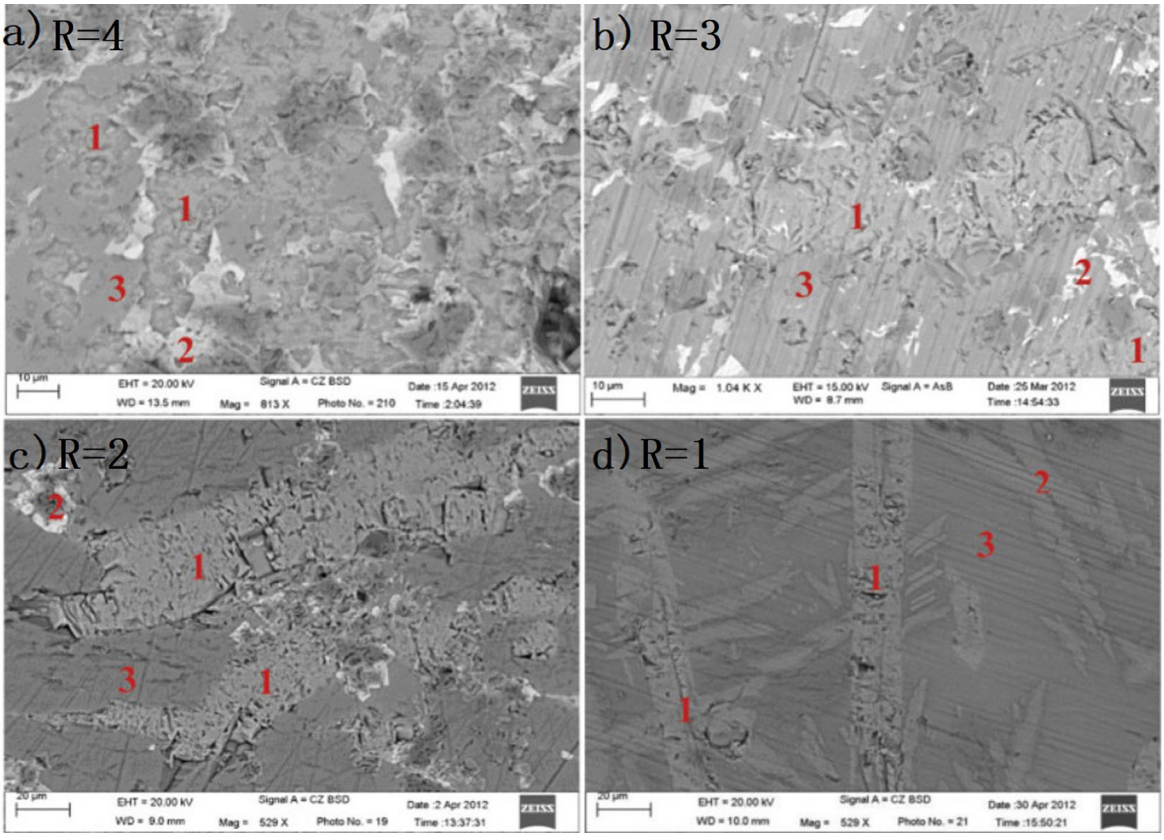

Fig. 16. Size of different phases (1: P-rich phase, 2: RO phase, 3: matrix phase) [8]

4.2. Effect of slag basicity and composition on selective growth and precipitation

Appropriate slag basicity and composition promote the selective growth and precipitation of the P-rich phase [8,9,15]. As shown in Fig. 16, the size of the P-rich phase is 10-30 μm, 20-100 μm, and 30-150 μm at R = 4, 3, and 2, respectively [8]. Further, the P-rich phase at R = 1 is rod-shaped and smaller than that at R = 2.

As MgO and MnO enter the RO phase, they have little effect on the selective growth and precipitation of the P-rich phase. Moreover, few studies have focused on the influence of P_2O_5 and Fe_tO contents on the selective growth and precipitation of phosphorus [9,15]. Zhou [9] has measured the size of the P-rich phase in CaO-Fe_tO-SiO_2-P_2O_5 slag. On increasing the P_2O_5 content from 6 wt% to 10 wt% and 18 wt%, the size of the P-rich phase increases from 20-60 μm to 30-90 μm and 50-80 μm, respectively.

4.3. Effect of additives on selective growth and precipitation

Recently, some studies focusing on the effect of additives (CaF_2, Na_2O, Al_2O_3, and TiO_2) on the selective growth and precipitation of the P-rich phase have found CaF_2 and Al_2O_3 have a positive effect [40,42]. According to Fig. 17a-b, the size of the P-rich phase is 20-40 μm on the addition of 3 wt% CaF_2 and increases to 100 μm on adding 6 wt% CaF_2 [40].

Jiang [42] has reported the effect of Al_2O_3 on the selective growth of the P-rich phase in CaO-SiO_2-Fe_2O_3-MgO-MnO-P_2O_5-Al_2O_3 slag. As shown in Fig. 18, the P-rich phase is significantly accumulated on the addition of Al_2O_3, and the size of the P-rich phase increases from 20 μm (without Al_2O_3) to 30-40 μm on the addition of 8 wt% Al_2O_3.

5. Separation of phosphorus from dephosphorization slag

5.1. Magnetic separation of dephosphorization slag

5.1.1. Effect of Slag Basicity and Composition on Magnetic Separation

A common method for separating dephosphorization slag is magnetic separation. The phosphorus recovery rate can be promoted under a suitable magnetic field intensity (<0.5 T) and slag size (<50 μm) [5,7,8,12,25,40,41,54-58]. Several parameters have been suggested to characterize magnetic separation [12].

$$L_P = \frac{\omega_{(P_2O_5)_1} \cdot M_1}{\omega_{(P_2O_5)_2} \cdot M_2} \tag{10}$$

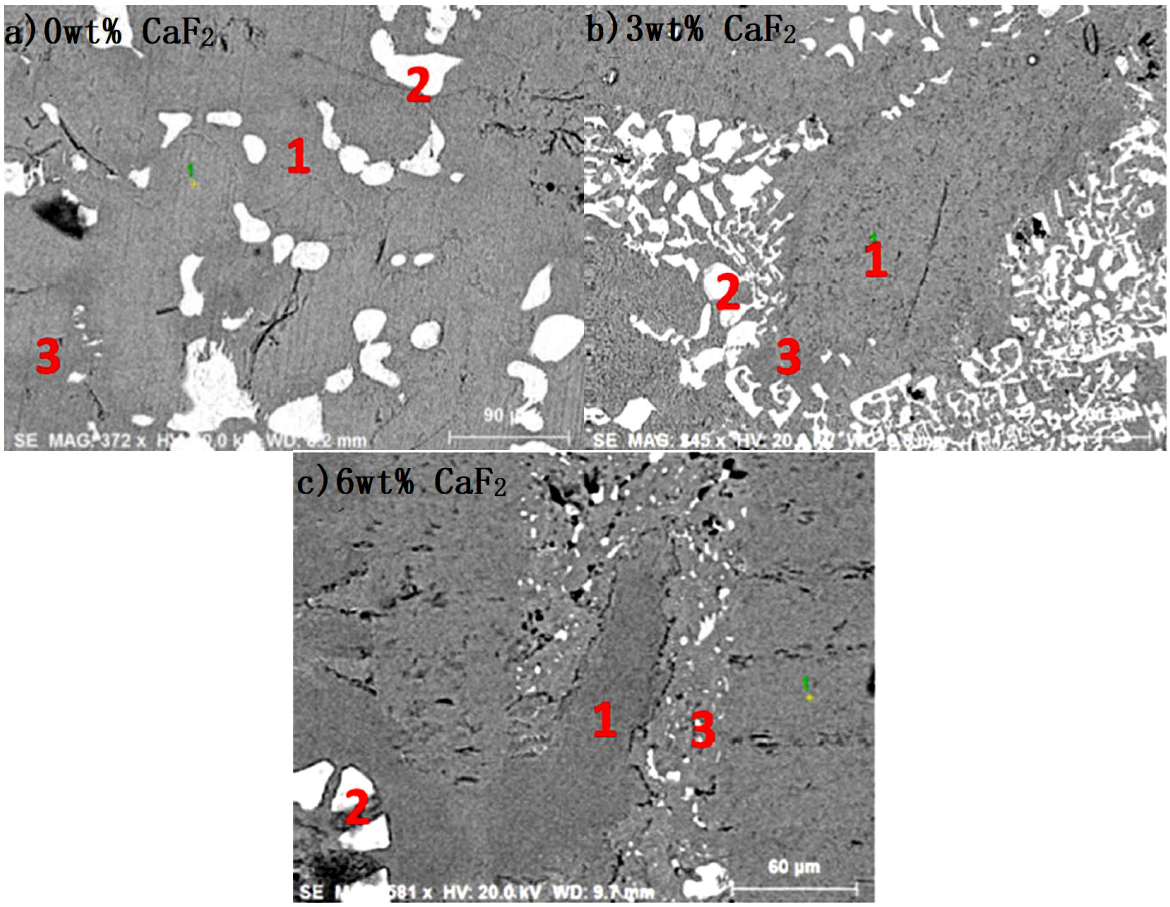

Fig. 17. Effect of CaF_2 on selective growth (1: P-rich phase, 2: RO phase, 3: matrix phase) [40]

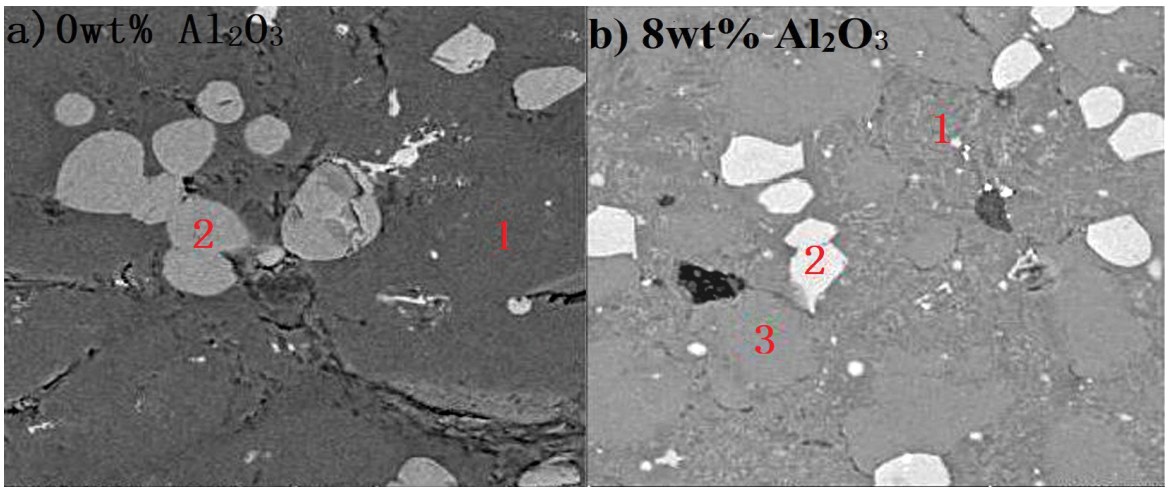

Fig. 18. Effect of Al_2O_3 on selective growth (1: P-rich phase, 2: RO phase, 3: matrix phase) [42]

$$H_{P,i} = \frac{\omega_{(P_2O_5)_1} \cdot M_1}{\omega_{(P_2O_5)_1} \cdot M_1 + \omega_{(P_2O_5)_2} \cdot M_2} \quad (i = 1 \text{ or } 2) \qquad (11)$$

$$H_{Fe,i} = \frac{\omega_{(TFe)_1} \cdot M_1}{\omega_{(TFe)_1} \cdot M_1 + \omega_{(TFe)_2} \cdot M_1} \quad (i = 1 \text{ or } 2) \qquad (12)$$

Where M_1 and M_2 are the mass of the nonmagnetic and magnetic substances (g), respectively; $\omega_{(P_2O_5)_1}$ and $\omega_{(P_2O_5)_2}$ are the mass fractions of P_2O_5 in the nonmagnetic and magnetic substances (%), respectively; L_P is the phosphorus partition ratio between the nonmagnetic and magnetic substances; $\omega_{(TFe)_1}$ and $\omega_{(TFe)_2}$ are the mass fractions of the nonmagnetic and magnetic substances (%), respectively; H_P is the P_2O_5 content (wt %) in the slag entering the nonmagnetic and magnetic substances; and H_{Fe} is the TFe content (wt %) in the slag entering the nonmagnetic and magnetic substances. The phosphorus recovery rate and iron recovery rate are defined by the P_2O_5 content entering the nonmagnetic substances and Fe content entering the magnetic substances, respectively.

Suitable slag basicity and compositions promote magnetic separation. Lin [12,15] has examined the effect of slag basicity on magnetic separation in CaO-SiO_2-Fe_tO-MgO-P_2O_5-MnO Al_2O_3/TiO_2/CaF_2 slag. When the R is decreased from 4 to 2, the P_2O_5 content in the slag entering the nonmagnetic substance increases from 64.59 wt% to 74.68 wt% and the L_P changes from 2.71 to 5.48. Moreover, as shown in Fig. 19, the phosphorus recovery rate increases from 73.5% to 84.57% when the R decreases from 4 to 2. Diao [58] has reported magnetic separation in CaO-10wt%SiO_2-Fe_tO-MgO-MnO-10wt%P_2O_5-Al_2O_3/TiO_2 slag (R = 2.5). According to Figure 18, the phosphorus recovery rate in the nonmagnetic substances is 74%.

MgO and MnO improve slag metallization and the magnetism of the iron-rich phase, resulting in the incomplete separation of phosphorus and iron [15,58]. As shown in Figure 18, on adding 10 wt% MgO and 10 wt% MnO to the slag, the phosphorus recovery rate in the nonmagnetic substances decreases from 65.44% to 40.43% and 35.8%. and L_P decreases from 2.71 to 0.63 and 0.56, respectively [15.] Diao [58] has added 10 wt% MnO into CaO-SiO_2-Fe_tO-MgO-MnO-10wt%P_2O_5 slag and has found that the phosphorus recovery rate decreases from 46% to 40%. Thus, the phosphorus recovery rate can exceed 70% when the slag basicity is 1.5-2.5. Further, MgO and MnO decrease the phosphorus recovery rate.

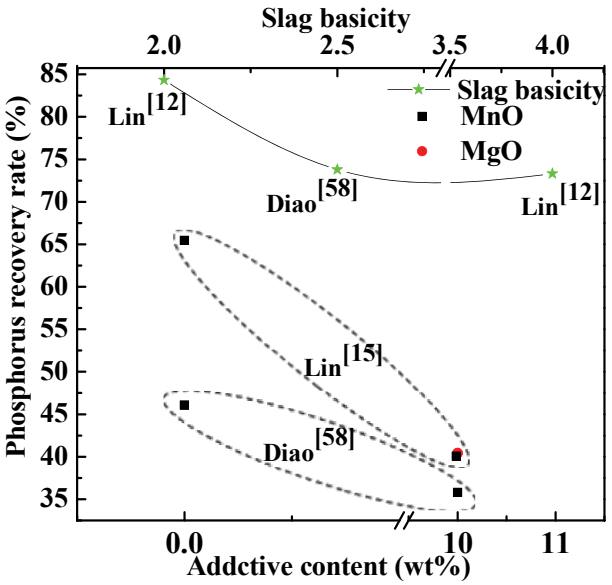

Fig. 19. Effect of slag basicity and compositions on magnetic separation

5.1.2. Effect of Additives on Magnetic Separation

Many studies [40-41,58] have revealed that CaF_2 and Na_2O improve slag metallization and the magnetism of the iron-rich phase. Moreover, they can result in the incomplete separation of phosphorus and iron. However, Al_2O_3 and TiO_2 are beneficial to magnetic separation .

Lin [40-41] has analyzed the phosphorus recovery rate in fluorine-free modified slag. As shown in Fig. 20, the phosphorus recovery rate is 64.6% in fluorine-free modified slag, while

it decreases to 48.8% on adding 6 wt% CaF_2. In addition, the phosphorus recovery rate is 64.55% on adding less than 6 wt% Na_2O, but it is only 36.53% on adding more than 6 wt% Na_2O. Therefore, the Na_2O content should be controlled to be within 6 wt%.

According to Fig. 21, the phosphorus recovery rate is 45.51 wt% in Al_2O_3-free slag and increases to 68.47 wt% and 82.16 wt% on increasing the Al_2O_3 content from 10 wt% to 15 wt%. Furthermore, the phosphorus recovery rate increases to 74.46 wt% on adding 10 wt% TiO_2. Additionally, the L_P is 4.61 and 2.91 on adding 10 wt% Al_2O_3 and 10 wt% TiO_2, respectively [12]. Simultaneously, Diao [58] has reported the effect of Al_2O_3 and TiO_2 on magnetic separation in CaO-SiO_2-Fe_tO-MgO-MnO-10 wt% P_2O_5 slag. The results reveal that the phosphorus recovery rate reached 87% and 70% on the addition of 10 wt% Al_2O_3 and 10 wt% TiO_2, respectively.

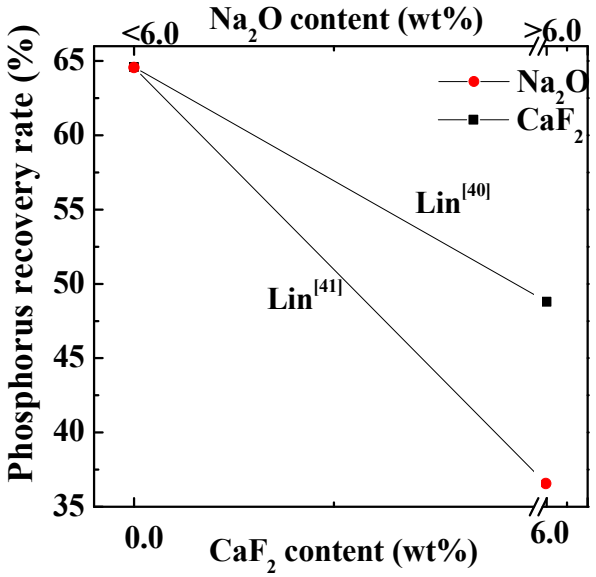

Fig. 20. Effect of CaF_2 and Na_2O contents on magnetic separation

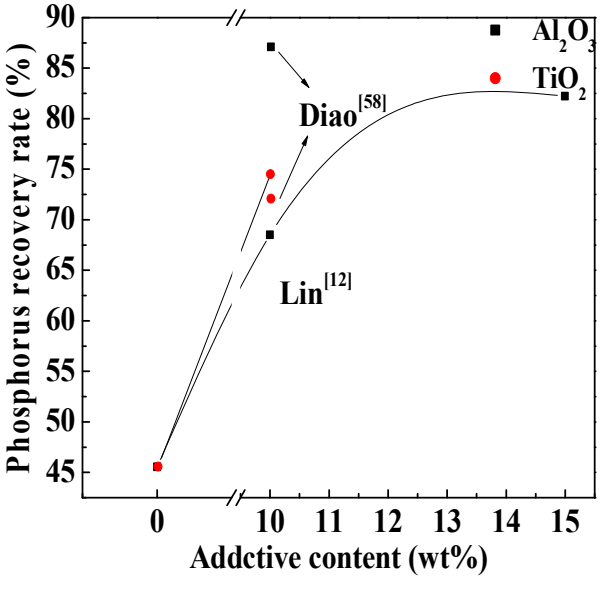

Fig. 21. Effect of Al_2O_3 and TiO_2 contents on magnetic separation

In summary, the phosphorus recovery rate increases to 60% either in fluorine-free modified slag or in slag containing 6 wt% Na_2O. Moreover, it reaches 70% on adding more than 10 wt% Al_2O_3 and 10 wt% TiO_2.

5.2. Separation of phosphorus from dephosphorization slag by supergravity separation

Previous studies have reported that calcium silicate in slag floats to the top due to the density difference between calcium silicate and the slag. Namely, CaO, SiO_2, and P_2O_5 accumulate at the top of the slag. Meanwhile, FeO, Fe_2O_3, and MnO accumulate at the bottom of the slag [48,49]. However, the initial temperature must be up to 1580°C and the average cooling rate should be less than $2°C \cdot min^{-1}$. Additionally, FeO and MnO contents must be more than 30% [48]. Supergravity separation has been found to be effective for phosphorus separation [50-53].

Li [50-52] has reported the separation of Fe-bearing and P-bearing phases in industrial slag. As shown in Fig. 22, the sample obtained by centrifugal enrichment (G = 800, T = 1663 K, t = 40 min) is compared with a parallel sample (G = 1, T = 1663 K, t = 40 min). According to Fig. 22a, a uniform structure is observed under normal gravity. However, an obvious stratified boundary appears after centrifugal enrichment (as depicted in the white line in Figure 21b). The bottom of the sample is compact and tight, while the top, where the P-rich phase is formed, is loose and porous [50]. Therefore , the enrichment efficiency is proportional to the centrifugation time and gravity coefficient.

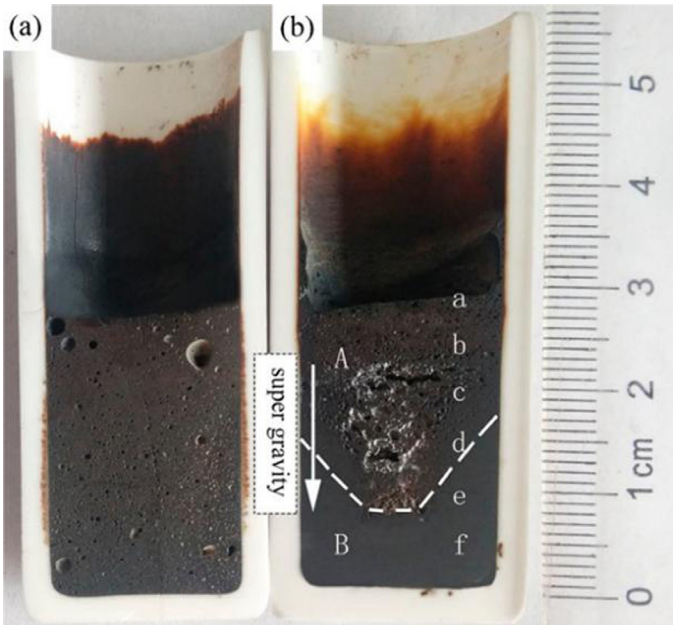

Fig. 22. Cross-section of the sample (a: parallel sample, b: sample after centrifugal enrichment) [50]

Li [50] has reported the separation of the Fe-bearing phase and P-rich phase in industrial slag (G = 800, T = 1663 K and

t = 40 min). The slag is fully mixed and 2 wt% CaF_2 is added. As shown in Fig. 23, the maximum mass fractions of P_2O_5 and Fe_tO in the P-rich and Fe-bearing phases are 4.12 wt% and 35.17 wt% and their recovery ratios are 77.56% and 60.18%, respectively. However, when G = 600, T = 1663 K, and t = 15 min, the mass fraction of P_2O_5 in the P-rich phase is 3.56 wt% and that of Fe_tO in the Fe-bearing phase is 38.67 wt% and the recovery ratios of P_2O_5 and Fe_tO are 82.2% and 68.5%, respectively [51]. Additionally, Li [52] has revealed the separation of P_2O_5 and Fe_tO in CaO-SiO_2-FeO-MgO-P_2O_5 slag (G = 700, T = 1623 K, and t = 20 min). The recovery ratios of P_2O_5 and Fe_tO are 76.67% and 85.02%, respectively. Gao [53] has also analyzed the separation of the Fe-bearing and P-bearing phases in high-phosphorous oolitic iron ore at 1200°C and G = 1200. The recovery ratios of P_2O_5 and Fe_tO are 99.19% and 95.83%, respectively.

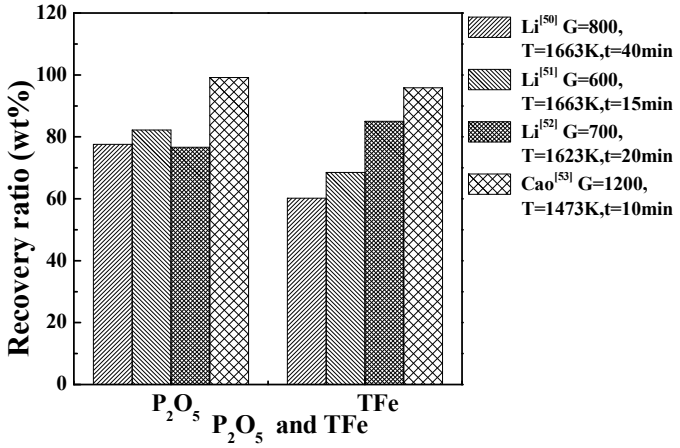

Fig. 23. Recovery ratio of P_2O_5 and Fe_tO

Consequently, the enrichment efficiency can be promoted by supergravity. Thus, the supergravity method is effective for the separation of the Fe-bearing and P-rich phases.

6. Summary and future applications

All the above studies have investigated the formation and evolution of phases in dephosphorization slag. Further, instructive data concerning the effect of various factors (slag basicity, slag composition, and additives) on the selective enrichment, growth, and separation of phosphorus have been obtained. However, most these studies have focused on laboratory investigations; therefore, the application in industrial production is still unclear.

Recently, the dephosphorization in hot metal pretreatment and previous stage of the steelmaking still utilize CaO-FeO-SiO_2 slag. The removal of phosphorus is thermodynamically favorable before decarburization because of the relatively low temperature. However, an increase in the dephosphorization efficiency is greatly limited due to the higher melting point and poor liquidity. Actually, Al_2O_3, Na_2O, and TiO_2 decrease the melting point and improve the liquidity. On the other hand, they replace parts of SiO_2 and combine with CaO to generate new phases (decreasing the value of "n" in $n$$C_2S$-$C_3P$). Therefore, the process not only effectively increases the P_2O_5 content in the P-rich phase but also promotes the magnetic separation of this phase. Further, Na_2O strengthens the magnetism of the Fe-bearing phase and has little effect on the magnetic separation. Li [61] has revealed that according to thermodynamics, Al_2O_3/TiO_2 slightly decreases the distribution ratio between the slag and carbon-saturated iron. However, according to semi-industrial test results, Al_2O_3/TiO_2 significantly improves the dephosphorization efficiency of the previous stage in the steelmaking process (before decarburization; [C] = 2.5-3.0%). The results show that the dephosphorization efficiency is up to 85% and the [P] content is less than 0.02% [62,63], which is beneficial to the smelting of medium and high-phosphorus-content hot metals. Additionally, it broadens the range of available iron ore resources and increases the purity of steel.

Therefore, CaO-FeO-SiO_2-Al_2O_3/TiO_2/Na_2O dephosphorization slag is significant for improving production efficiency and resource utilization. Previous studies have analyzed the behaviors of phosphorus enrichment and separation under the conditions of thermodynamics/dynamics. To effectively increase the practical application of dephosphorization slag, further research concerning phosphate fertilizers are necessary. Although Al_2O_3/TiO_2/Na_2O enriches the P-rich phase, how the proportion of the P-rich phase in dephosphorization slag changes with different compositions directly affects the total P_2O_5 solubility in the slag. Moreover, few investigations have focused on the most direct data related to the quantity of dephosphorization slag. The P_2O_5 content in the slag increases with increasing dephosphorization efficiency. However, the variation in slag viscosity and slag structure caused by P_2O_5 content affects the liquidity and separation of the slag. Therefore, further studies on these aspects should be conducted.

Acknowledgement

The authors would like to thank the National Natural Science Foundation of China (No. 51474021) for financial support.

REFERENCES

[1] S. Jung, Y. Do, J. Choi, Steel Res. Int. **77** (2006).
[2] H. Ono, A. Inagaki, T. Masui, N. Hiroshi, N. Shoji, ISIJ Int. **21** (2), 135-144 (1980).
[3] H.J. Li, ISIJ Int. **35** (9), 1079-1088(1995).
[4] Z.J. Wang. Investigation on Physical and Chemical Properties of P-bearing Steelmaking Slags during the Selective Enrichment Process of Phosphorus. PhD thesis, University of Science & Technology Beijing, June.
[5] Z.T. Sui, B.C. Chen, in: Proceedings of the National Powder Engineering Conference, China 1998.
[6] Z.T. Sui, T.P. Lou, N.X. Fu, CN1253185, China 2000.

[7] J.Y.Li. Selective enrichment and phase separation of phosphate in steelmaking slags. PhD thesis, University of Science & Technology Beijing, December.

[8] L. Lin, Y.P. Bao, M. Wang, Ironmaking and Steelmaking **40** (7), 521-527 (2013).

[9] H.M. Zhou, Y.P. Bao, L. Lin, China Metall. **23** (1), 45-49 (2013).

[10] S. Ken-Ichi, K. Shin-Ya, H. Shibata, Tetsu-to-Hagane **49** (49), 505-511(2009).

[11] H.M. Zhou, Y.P. Bao, L. Lin, Steel Res. Int. **84** (9), 863-869 (2013).

[12] L. Lin, Y.P. Bao, M. Wang, Ironmaking and Steelmaking **21** (5), 496-502 (2014).

[13] L.C. He, Y.M. Wang, Fertilizer industry knowledge, 1975, Fuel Chemical Industry Press, Beijing(in Chinese).

[14] H.G. Jin, L.B. Yu, China Res. Comp. Util. **3**, (1999).

[15] L. Lin, Y.P. Bao, M. Wang, High Temp. Mater. Proc. **35** (4), 425-432 (2016).

[16] L. Lin, Y.P. Bao, M. Wang, ISIJ Int. **54** (12), 2746-2753 (2014).

[17] J. Diao, L. Jiang, Y. Wang, Phosphorus Sulfur **190** (3), 387-395 (2014).

[18] L.S. Li, X.F. Yu, X R. Wu, P. Soc. Photo-Opt. Ins. **10** (1), 78-81 (2006).

[19] L.S. Li, X.F. Yu, China Metal. **17** (1), 42-45 (2007).

[20] S. Fukagai, T. Hamano, F. Tsukihashi, ISIJ Int. **47** (1), 187-189 (2007).

[21] X. Yang, H. Matsuura, F. Tsukihashi, Metal. Mater. Trans. B **51** (9), 1298-1307 (2010).

[22] H.J. Guo, Metallurgical Physical Chemistry Tutorial, 2006, Metallurgical Industry Press, Beijing(in Chinese).

[23] X.G. Wu, J.N. An, J. Anhui Univ. Technology **27** (3), 233-237(2010).

[24] H. Ono, Tetsu-to-Hagane **3**, (1980).

[25] K. Ito, M. Yanagisawa, N. Sano, Tetsu-to-Hagane **6**8 (2), 342-344 (1982).

[26] N. Wang, Z.G. Liang, M. Chen, Northeast Univ. J. **32** (6), 814-817 (2011).

[27] X.F. Dou, M.M. Zhu, T.C. Lin, Chongqing Univ. J. **38** (5), 78-82 (2015).

[28] X. Yang, H. Matsuura, F. Tsukihashi, ISIJ Int. **49** (9), 1298-1307 (2009).

[29] X. Yang, H. Matsuura, F. Tsukihashi, ISIJ Int. **50** (5), 702-711 (2010).

[30] X. Yang, H. Matsuura, F. Tsukihashi, Tetsu-to-Hagane **95** (95), 268-274 (2009).

[31] H. Suito, R. Inoue, T. Iron Steel I. Jpn. **46** (2), 180-187 (2006).

[32] R. Inoue, H. Suito, ISIJ Int. **46** (2), 174-179 (2006).

[33] C. Su, L.Z. Chang, in: Proceedings of the National Metallurgical Energy Environmental Protection Production Technology Association, China 2014.

[34] M.C. Jha, G.R. Wicker, US4110400, US 1978.

[35] P. Zhang, Z. Sui, Metall. Metal. Mater. Trans. B **26** (2), 345-351 (1995).

[36] P.K. Son, Y. Kashiwaya, Tetsu-to-Hagane **48** (9), 1165-1174 (2008).

[37] X.M. Yang, J.P. Duan, C.B. Shi, Metal. Mater. Trans. B **42** (4), 738-770 (2011).

[38] X.M. Yang, C.B. Shi, Z. Meng, Metal. Mater. Trans. B **42** (1), 951-977 (2011).

[39] Y.Liu, Q.F. Shu, Nonferrous Metal. Sci. Eng. **7** (3), 29-34 (2016).

[40] L. Lin, Y.P. Bao, Q. Yang, Ironmaking and Steelmaking **42** (3), 331-338 (2015**)**.

[41] L. Lin, Y.P. Bao, W. Jiang, ISIJ Int. **55** (3), 552-558 (2015).

[42] L. Jiang, J. Diao, X.M. Yan, Proceedings of the National Powder Engineering Conference, China 2014.

[43] X.L. Pan, J.Y. Li, M. Guo, J. Iron Steel Res. **29** (6), 474-480 (2017).

[44] L. Jiang, J. Diao, X.M. Yan, ISIJ Int. **55** (3), 564-569 (2015).

[45] L. Lin, Y.P. Bao, M. Wang, Chinese J. Eng. **8** (1), 1013-1019 (2014).

[46] Z.M. Wang. The Study on the Separation and Growing up of Perovskite Phase from the Blast Furnace Slag Containing Titanium. PhD thesis, Northeastern University, June.

[47] G.M. Yang, X.R. Wu, L.S. Li, Can. Metall. Quart. **51** (2), 150-156 (2012).

[48] H. Ono, A. Inagaki, T. Masui, ISIJ Int. **21** (2), 135-144 (1980).

[49] H. Ono, A. Inagaki, T. Masui, H. Narita, Tetsu-to-Hagane **66** (9), 1317-1326 (1980).

[50] C. Li, J.T. Gao, F.Q. Wang, Ironmaking and Steelmaking, 1-6 (2016).

[51] C. Li, J. Gao, Z. Wang, ISIJ Int. **57** (4), 4 (2017).

[52] C. Li, J. Gao, Z.C. Guo, Metal. Mater. Trans. B **47** (3), 1516-1519 (2016).

[53] J. Gao, Y. Zhong, L. Guo, Metal. Mater. Trans. B **47** (2), 1080-1092 (2016).

[54] K. Yokoyama, H. Kubo, K. Mori, T. Iron Steel I. Jpn. **47** (10), 1541-1548 (2007).

[55] H. Kubo, M.Y. Kazuyo, T. Nagasaka, T. Iron Steel I. Jpn. **50** (1), 59-64 (2009).

[56] X.R. Wu, G.M. Yang, L.S. Li, Ironmaking and Steelmaking **41** (5), 335-341(2014).

[57] M.Y. Kazuyo, Trans. T. Iron Steel I. Jpn. **50** (3), 306-312 (2010).

[58] J. Diao, B. Xie, Y. Wang, ISIJ Int. **52** (6), 955-959 (2012).

[59] Y.H. Wang, B. Xie, J. Diao, Chinese J. Eng. **33** (3), 323-327 (2011).

[60] Z.H. Xu, Steel slag phosphate fertilizer production, 1962, China Industry Press, Beijing (in Chinese).

[61] F.S. Li, X. Li, Y.L. Zhang, Metal. Mater. Trans. B **48** (5), 1-12 (2017).

[62] F.S. Li, Y.L. Zhang, Z. Guo, JOM-Us **69** (2), 1624-1631 (2017).

[63] F.S. Li, Y.L. Zhang, Z. Guo, JOM-Us **69** (9), 1632-1638 (2017).